

## Fibre reinforced composite dental bridge. Part II: numerical investigation

W. Li<sup>a,\*</sup>, M.V. Swain<sup>a,b</sup>, Q. Li<sup>c</sup>, J. Ironside<sup>b</sup>, G.P. Steven<sup>d</sup>

<sup>a</sup>*School of Aerospace, Mechanical and Mechatronic Engineering, The University of Sydney, City Road, Sydney, NSW 2006, Australia*

<sup>b</sup>*Faculties of Dentistry, The University of Sydney, Sydney, NSW 2006, Australia*

<sup>c</sup>*School of Engineering, James Cook University, Townsville, QLD 4811, Australia*

<sup>d</sup>*School of Engineering, University of Durham, Durham, DH1, 3LE, UK*

Received 3 September 2003; accepted 27 December 2003

### Abstract

Motivated by the clinical success and limitations on experimental investigation of the fibre-reinforced composite dental bridge, this paper aims at providing a numerical investigation into the bridge structure. The finite element (FE) model adopted here is constructed from computer tomography images of a physical bridge specimen. The stress and strain distributions in the bridge structure especially in the bonding interfaces are analyzed in detail. The peak stresses and their variations with the different bridge designs are evaluated. Due to the lower bond strengths of adhesives and the high stress concentration in the pontic–abutment interface, the likelihood of failure in the interface is predicted by finite element analysis. The validity of the numerical results is established by a good agreement between the FE prediction and the tests in the load–deflection responses, the structural stiffness as well as the failure location of the composite dental bridge.

© 2004 Elsevier Ltd. All rights reserved.

**Keywords:** Finite element; Dental biomaterials; Failure analysis; Unilateral contact

### 1. Introduction

Clinical observations and experimental investigations have shown that, for the direct composite resin-bonded bridge structures, debonding at the interface between the abutment and pontic reflects a major mode of failure [1–3]. An unexpected interfacial debonding can lead to entire failure of the bridge, even though the reinforced-fibre may prevent the pontic from dismounting completely. Therefore, the knowledge about the adhesion strength, initiation and progression of debonding is of prime importance as suggested from the clinical observations [2,4,5].

Since mechanical failure is mainly caused by excessive stresses or deformation, a full understanding of stress fields developed in the dental bridge becomes particularly significant. As the most representative numerical method, finite element analysis (FEA) is considered suitable to model such structures as the dental bridge,

where there are highly irregular geometry, diverse design variations, complex load/boundary conditions, as well as non-linear and orthotropic material behaviours. More importantly, FEA allows quantifying specific stress and displacement distributions anywhere within the analysis domain, which can be very difficult (if not impossible) by means of analytical or experimental methods. Additional advantage of finite element (FE) modelling is its powerful capability of parametric studies. Once the fundamental FE model is appropriately verified, it could conveniently evaluate the influence of geometry and parameter variations such as shape, materials properties, boundary conditions, etc.

In the past two decades, there have been some publications devoted to the FE stress analysis of various dental bridges. In 1989, Farah et al. [6] developed two-dimensional FEA to examine the principal stresses due to the placement of three- and four-unit bridges in a mandibular quadrant model. To determine the stress and displacement fields, Yang and Thompson [7] also presented FE model for the three- and four-unit bridges in a mandibular posterior segment. In 1992, Awadalla et al. [8] introduced a simplified 3D FE model to

\*Corresponding author. Tel.: +61-2-9351-7129; fax: +61-2-9351-4841.

E-mail address: [wei@aeomech.usyd.edu.au](mailto:wei@aeomech.usyd.edu.au) (W. Li).

evaluate the stress field in a cantilever fixed partial denture. Yang et al. [9] adopted a 2D FE model to investigate the mechanical behaviour of a cantilevered fixed partial denture with normal and reduced bone support. Unfortunately, little existing FEA has involved the direct composite fibre-reinforced dental bridge structures.

This study provides a 3D FEA to evaluate the structural responses of the dental bridge with design variations of fibre number and boundary conditions. The locations and magnitudes of the stress concentrations that occur with the different bridge designs are identified. The numerical predictions of the locations of stress peaks, structural stiffness and failure modes are compared with those experimental observations. As part of on-going project towards an automatic analysis and design, the 3D bridge model is generated from computer tomography (CT) images of a physical specimen and upon reference to average tooth dimensions in this paper [10]. The discrete accuracy of FEs is then verified by a convergence test and the validity of modelling is established by laboratory tests.

## 2. Materials and methods

### 2.1. Three-dimensional FE model

A physical model of a two-unit cantilever composite fibre-reinforced dental bridge is adopted as the basis of the specimens to be tested and the 3D FE models to be analyzed. The dental bridge consists of an artificial maxillary left incisor made of composite bonded by adhesive to a natural maxillary right incisor. The structure is reinforced by either the polyalkane or polyethylene fibre(s) (whichever available in clinic) with a high elastic modulus.

In this study, a non-destructive CT scan technique (GE9800) is employed to accurately acquire the geometrical data from the physical model of the bridge. To yield a reasonable geometric accuracy for three-dimensional reconstruction, the bridge is spaced with a uniform interval of 1.0 mm. Consequently, 24 serial CT sectional scans are obtained from the abutment tooth apical root to incisal edge. The raw CT scan data is subsequently fitted to a continuum mathematical model by means of NURBs [11] in EDS Unigraphics system (Sun Sparc). Then, the FE mesh is generated with an in-house program. The entire procedure includes several main steps of data acquisition, image processing, geometry reconstruction and mesh generation.

Since tooth dimensions differ widely from individual to individual, to ensure the model more representative, appropriate modifications for some surface points are introduced from the average dimensions of the tooth structures [10]. In the real model, the fibre(s) is covered

by a resin composite to produce a smooth surface. Since this coverage has relatively little contribution to the strength of the bridge compared with the fibre, it is neglected from the FE modelling in this study.

Clinically the thickness of an adhesive layer in the pontic–abutment interface varies from 0.02 to 0.1 mm [12], which appears fairly difficult to be accurately modeled unless an unrealistically fine mesh is used. A pilot study has revealed that although there are noticeable deviations (displacement > 15% and interfacial peak stress > 35%) between the models without and with considering interfacial adhesive layer, the differences between the adhesive thicknesses of 0.1 and 0.2 mm are relatively small [13]. Considering the appropriateness of geometrical aspect ratio, an adhesive layer with a 0.2 mm thickness is modelled to investigate the stress field developed in the pontic–abutment interface.

The fundamental bridge model consists of five different material parts: (1) abutment dentin, (2) crown (enamel), (3) composite pontic, (4) reinforced fibre and (5) adhesive layers on abutment/pontic, abutment/fibre and pontic/fibre interfaces. The pilot study also shows that the root of the abutment (dentin) has a less geometric complication and develops lower stress concentrations compared to the crown and connecting parts in the bridge. Thus a coarse mesh is allocated in the root and a dense mesh over the other parts of the bridge model.

To evaluate the discrete accuracy of the FE model, four three-dimensional FE meshes of the fundamental bridge model, with increasing numbers of nodes and elements, are constructed to perform a convergence test. The mesh size varied from mesh 1 with 245 elements (4077 dof), mesh 2 with 674 elements (10,086 dof), mesh 3 with 1362 elements (20,397 dof) to mesh 4 with 2337 elements (32,072 dof). All models have assigned the same material properties and the same loading condition. Simplified boundary conditions are applied, where the bone structure that supports the root is assumed to be rigid while the periodontal ligament between the bone structure and the root is neglected. The convergence of the FE model is evident in the curve of the maximum upward displacement of the models [13]. Considering both accuracy and computational efficiency, mesh 3 with around 21,000 degrees-of-freedom is adopted as the mesh size with an appropriate accuracy for subsequent multiple FEA analyses on the various bridge arrangements of this study.

### 2.2. The loading, boundary conditions and material properties

In general, a tooth structure does not stand alone. Each tooth is in static and dynamic contact with its neighbors at each side of it as well as with the opposing

teeth. Normally, there exists at least a  $13\ \mu\text{m}$  clearance space [9] between adjacent teeth. When such a  $13\ \mu\text{m}$  clearance space is closed due to a certain level of compressive bite force, a positive contact relationship between the adjacent teeth and dental structure can be developed. Under such a situation, the dental structure would be partially supported by the contact forces coming from its neighboring teeth [13].

In order to accurately quantify the effects of the adjacent teeth on the bridge structural response, this study introduces a unilateral contact boundary condition to model the interaction between the bridge and the adjacent teeth by means of *compression only gap contact* elements [14]. The gap element is designed to transmit compressive force only when the adjacent teeth are in contact with the bridge. A number of compression gap elements are installed on the proximal surface where the potential contact likely takes place. Considering the material properties of the adjacent teeth, an averaged modulus between bridge materials and the adjacent teeth is assigned to the gap elements. The 3D FE model of the bridge with the unilateral contact boundaries is illustrated in Fig. 1.

Whereas in the laboratory experiment, the abutment tooth, which is made by cementing a cast brass core and a porcelain jacket crown together, is supported by a special model resin cast (DVA Polyroqq die and model resin) and cured tray resin [3]. To describe such a physical situation more accurately, an extra region of FE mesh to incorporate part of the DVA and tray resins is added as shown in Fig. 1. For further study, a layer of special mesh is also arranged to model the periodontium tissue around the tooth root, but its material property is

assigned as the same as the one of bone/base materials at this stage. Thus, the final model consists of 1761 elements and 9102 nodes for the double-fibre design with the adjacent teeth. The elements used are mostly twenty-node quadratic hexahedral brick elements and some fifteen-node quadratic wedge elements to better capture the complex curved boundaries/interfaces of the abutment, composite pontic and the fibre(s). In addition, a number of gap elements (here eight on each side) are placed to simulate the unilateral contact or non-contact situation on the proximal surface between the bridge and the adjacent teeth. The sectional surfaces in alveolar bone or base structure, which is considered kinematically far away from the bridge's abutment and the deformation becomes fairly small, are fully clamped as illustrated in Fig. 1. But the facial and lingual surfaces of the alveolar bone or base structure are set completely free for modelling the real situation.

In this study only linear elastic behaviour is considered and a concentrated bite force of 100 N is applied at the four different positions, as in the experiments (refer to Fig. 1). It is further assumed that the bite force is oriented at  $26^\circ$  to the vertical axis ( $x$ -axis herein) that represents the angle at the first contact of tooth during biting [15,16].

Although fibres generally exhibit transversely isotropic behaviour [17], they are treated as isotropic in the analysis due to their negligible effect on the structural responses (relative errors are less than 0.1% in stress peaks and deflection, respectively [13]). To enable comparison with the experimental results, the properties of the cast brass, porcelain and cured tray resin are assigned, respectively, to the mesh of dentin, enamel and alveolar bone structure in the FEA models. For simplicity and also owing to the fundamental lack of precise biomaterial information, all material properties are assumed isotropic in this study, as listed in Table 1.

To identify the role that the fibres could play in the structural responses, the single-fibre and double-fibre designs are modeled as shown in Figs. 2(a) and (b), respectively. Taking into account the unilateral boundary conditions with and without the adjacent teeth, consequently, four FE models are analysed altogether. The FE computing is performed by using package Strand7 [14] in a Pentium IV PC (1.7 GHz with 1 GB RAM).

### 3. Results and discussions

#### 3.1. Principal stress peak and location

Since the overall stiffness and the peak stresses reflect the major concerns of the structural performance and failure analysis, the principal stress peaks in the bridge,

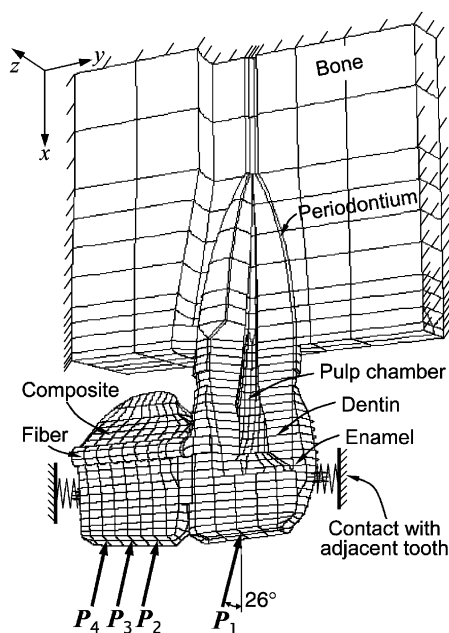


Fig. 1. 3D FE model of the dental bridge structure.

Table 1  
Material properties used in the analysis

Material	Young's modulus (MPa)	Poisson's ratio
Porcelain [18]	68,900	0.28
Cast brass [19]	18,000	0.31
Cured tray resin [13]	13,700	0.30
Fibre [20]	50,000	0.30
Adhesive [20]	2000	0.30
Composite [20]	18,000	0.30

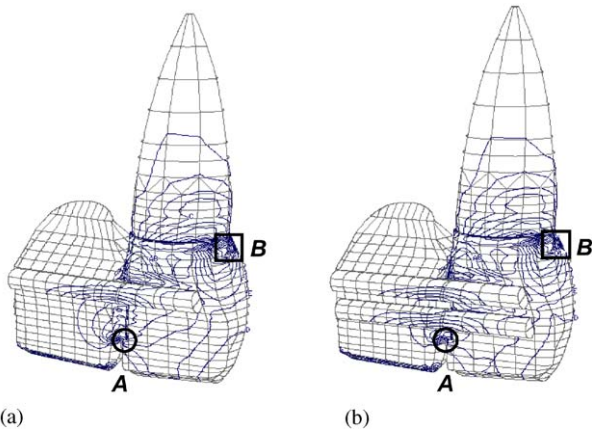


Fig. 2. Contours of principal tensile stress  $\sigma_{11}$ : (a) single fibre design and (b) double fibre design.

Table 2  
Comparisons of the principal stress peaks  $\sigma_{11}^a$  in the adhesives,  $\sigma_{11}^b$  in the entire bridge (MPa) and displacements  $u_x$  (mm) under load  $p_3 = 100$  N

Designs	With adjacent teeth			Without adjacent teeth		
	$\sigma_{11}^a$	$\sigma_{11}^b$	$u_x$	$\sigma_{11}^a$	$\sigma_{11}^b$	$u_x$
Single fibre	28.10	50.67	0.0784	33.57	65.22	0.08326
Double fibre	25.55	50.59	0.0771	30.60	65.37	0.08250

the adhesive and the upward displacement by FEA for all models are tabulated in Table 2.

Unsurprisingly, the principal stress peaks occur in the high stress concentration areas as marked in circles and squares in Fig. 2. The magnitudes of the principal stress peaks and the displacements differ from the design variations. As summarized in Table 2, the contribution of adjacent teeth, fibre number and the bond in the pontic–abutment interface to structural response could be made clear by detailed analysis of the results. For example, the maximum principal stresses and the displacements in the bridge could be reduced by about 23 and 6%, respectively, by considering the effect of adjacent teeth to the single- and double-fibre designs. It reveals that the loading on the bridge is substantially

shared by the adjacent teeth contacted. To a certain extent, this convincingly demonstrates the significance for dentists to best possibly use the adjacent teeth as load supporter when constructing the bridge.

It is interesting to note that the number of the fibre(s) has almost no influences in the maximum principal stresses and structural stiffness in the bridge. This indicates that the pontic is mostly supported by the bond on the pontic–abutment interface and the adjacent teeth, whereas the fibre(s) only acted as an over-constraint with insignificant contribution to such overall mechanical responses. However, the effects of fibre number on the failure loads and deflections appear more remarkable in the experiment [3]. It could be explained as that in the numerical analysis, the interface between the abutment and pontic is assumed bonded perfectly, while in the experiment, diverse manufacturing flaws existed in the adhesive layer could make the bond weaker and the reinforced fibre(s) would partially support the bridge.

It should be pointed out that although there is a principal stress peak over the entire bridge observed on the crown distal surface near the cervical line of the abutment (location B as squared in Figs. 2(a) and (b)), it is not counted as a failure stress because the strength of abutment is generally much higher than those in the connector of the bridge. Instead, the other stress concentration in location A (as circled in Figs. 2(a) and (b)), in spite of a smaller magnitude, may indicate a higher possibility of failure due to the lower strength in adhesives. To more specifically explore the stress distribution patterns in the bonded interfaces, Fig. 3 plots the tensile stress contours within the adhesive layers. It can be clearly seen that there are higher stress gradients in the incisal part of the adhesive as circled in Fig. 3.

With regard to the failure loads, the effects of the fibre number and the adjacent teeth on the principal stress peaks  $\sigma_{11}^a$  in the adhesive interface seem noteworthy (respectively by around 10% and 16%), which to some extent reflects the contributions of fibre number and the adjacent teeth to the failure strength. Indeed, the peak stress calculations within the adhesive layer provide essential information for the analysis of the failure process. If the tensile and shear bond strengths between etched enamel and composite are considered as 20 MPa [21,22], then the numerical results (from Table 2) imply that the bonding interface is a potential failure location as that the predicted tensile and shear stress peaks have exceeded the corresponding bond strengths in the interface. In fact, experimental observations also provide evidence that the failures cohesively initiate from incisal portion in the enamel–adhesive–composite interfaces but with a higher loading level [3]. Undoubtedly, this emphasizes the importance of modelling and evaluating the stress status in the adhesive.

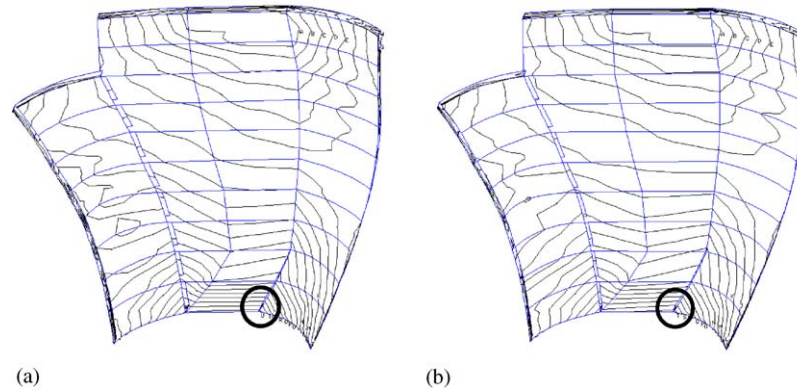


Fig. 3. Contours of principal tensile stress  $\sigma_{11}$  in adhesive layer in the pontic–abutment interface: (a) single fibre design and (b) double fibre design.

However, it must be pointed out that in the material tests the bond strength represents the ratio of the load at which the bond fractures to the cross-sectional area of the bond. This provides an average measure in a uniaxial stress status but does not consider the stress gradient and complex stress status. In fact, the failure may not occur even though the stress peaks have exceeded the bond strength. The mechanism is indeed quite complex here. Also, many factors, including the dentine substrate, the storage conditions and the test method, would affect the bond strength values. This calls for a more specific study in the mechanism of adhesive failure in such complex components as the dental bridge, but this is beyond the scope of this study. In Ref. [23], the crack propagation path in the adhesive layer can be approximately identified using fracture mechanics methods by using the FE stress data.

In addition, because of the approximation in the FE modelling of the adhesive interface, the numerical results should not be interpreted in a strictly quantitative sense. Although the higher order interpolations by a 20-node FEs has been adopted, a poor elemental aspect ratio (modelling the 0.2 mm adhesive layer) could in effect result in considerable numerical errors due to adopting a thicker adhesive layer to represent the bonding material and implementing a coarse mesh near the interface. If it is possible to further reduce the thickness of the adhesive layers and refine the interfacial mesh, such modelling and numerical errors could be reduced and FEA would therefore be more accurate.

### 3.2. Numerical and experimental comparisons

#### 3.2.1. Failure mode and location

The comparison of failure location between the test and FEA is illustrated in Fig. 4. From the tensile stress contour shown in Fig. 4(a), a high principal tensile stress ( $\sigma_{11}$ ) concentration around region A is clearly observed. It implies that the fracture most likely originates from

the incisal portion in interface adhesive because of the significant stress concentration associated with the notch.

In a clinical study of the direct composite bridges, Culy and Tyas [2] reported that the failure usually took place at the enamel–resin interface for the cohesive resin composite. From the experimental investigation in the companion paper [3], it is also observed that failure in most of the specimens are resulted from a stable fracture originating along the interface between the abutment and the pontic (the porcelain–composite resin bond), as illustrated in Fig. 4(b). Thus the FEA prediction on the failure location is consistent with the clinical and correlates with the experimental observations.

#### 3.2.2. Load–deflection curves

A series of 0–100 N load–deflection curves from the experimental measurements is plotted and compared with those predicted by FEA. Taking the double-fibre design as an example, the curves of loading–deflection for both the experiment and FEA are plotted in Fig. 5, in which these four curves, respectively, depict four different loading positions as illustrated in Fig. 1.

An obvious difference observed is a non-linear behaviour at the beginning of the load processes during the experiment. It can be due to a fact that the initial force acts to eliminate the contact gaps between the loading unit and the specimen as well as between the bottom of the specimen and the platform of the machine. Such a non-linear phenomenon persists until all gaps come into contact. Subsequently, a linear relation between the displacement and load can be approximately identified. This indicates that the structural behaviour for such a dental bridge performs mainly linearly except for the above-mentioned initial non-linear portion. Thus an elastic FE simulation for the structure is somewhat acceptable.

The comparison of the load–deflection curves also shows that the experimental deflection values are larger

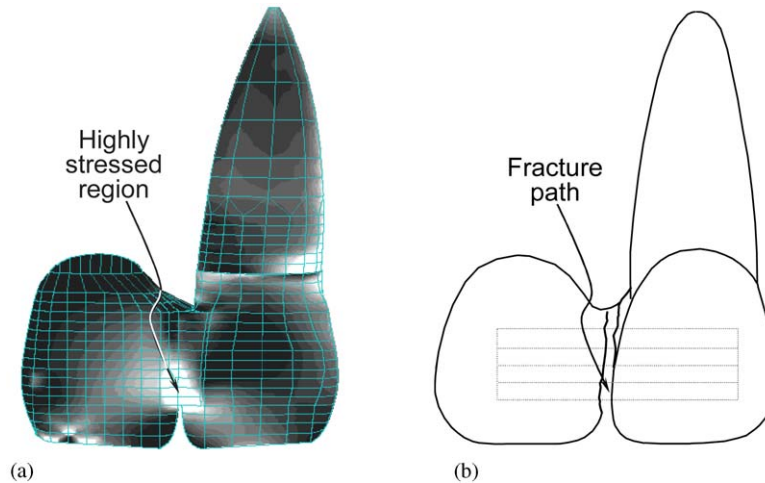


Fig. 4. Comparison of failure location between FEA and test: (a) tensile stress contour from FEA and (b) failure location in experiment.

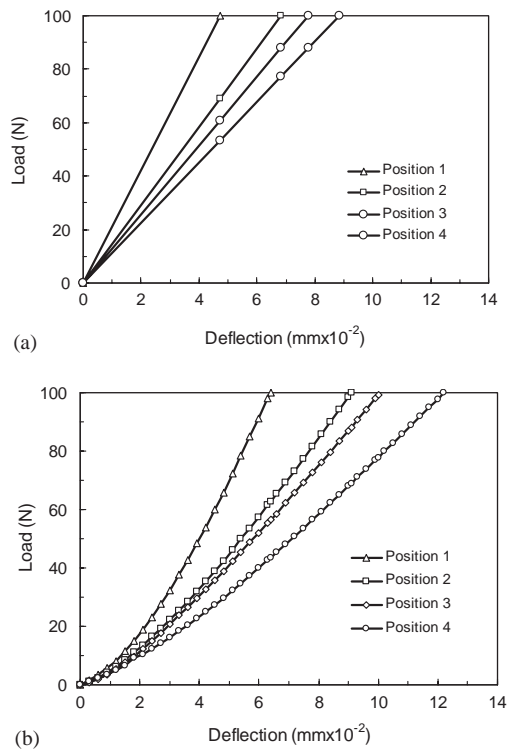


Fig. 5. Comparison between the FEA and the test for double fibre design: (a) FEA prediction and (b) experimental data.

than those predicted by the FEAs. It is easy to appreciate that the contact gap mentioned above is one of the reasons. At the same time, the deformations of the loading unit and angle fixture at loading would all considerably contribute to the total deflection in the tests. While in linear FEA such initial gaps as well as the deformations in the loading unit and plastic angle fixture are disregarded. This calls for a detailed non-linear FEA in future study.

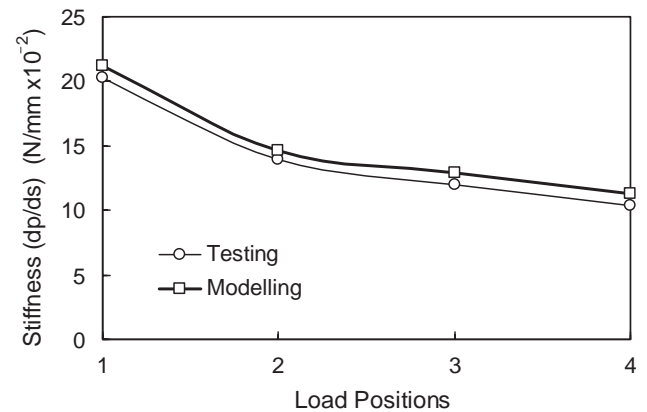


Fig. 6. Slopes of load–deflection curves for the double fibre design.

To distinguish the initial non-linearity and unaccounted deformations, the slopes (i.e. structural stiffness) of the linear portion of the load–deflection curves for the experiment, in the load range of 50–100 N, are compared with those by FEA in Fig. 6. A good agreement can be clearly identified for all of the four loading locations. The differences of stiffness between corresponding curves are 4.1%, 4.8%, 6.1% and 8.8% at load positions 1, 2, 3 and 4, respectively. Apart from the effect of unaccountable deformations mentioned above, errors in specimen manufacturing and assembling may also add to these differences. Considering the uncertainties and assumptions regarding the exactness of the modelling, this comparison appropriately verifies the reliability of the computational stiffness for the bridge structure.

#### 4. Concluding remarks

This study aims at exploring the fundamental mechanical responses of the direct resin-bonded dental

bridge structures. The 3D quadratic FE model is developed by means of a procedure from the CT scan data to a continuum mathematical model and further to the discrete elements. The discretization accuracy of finite elements (FEs) is assessed by the convergence test and the analysis validity of the model is established by the laboratory test.

The numerical analysis of the bridge structure reveals that a high stress concentration occurs around the incisal portion of the adhesive interfaces between the pontic and abutment. The magnitudes of these stress concentrations and their variations with the different bridge designs are compared. It is known that the influences of adjacent teeth seem significant for both the stress and stiffness, whereas the fibre(s) acts as an auxiliary component only. It is the adhesive interface between the abutment and pontic that plays the most crucial role in supporting the pontic. Considering the lower tensile and shear bond strengths of adhesives, the FE results demonstrate that the crack most likely initiates from the incisal portion in adhesive interface of the pontic–abutment.

A good agreement between the FE prediction and the experimental results is noted in the overall stiffness and the failure location of the dental bridge. On the one hand, this agreement establishes confidence in the validity of the numerical results. On the other hand, it shows once again that finite element analyses are an important complement to laboratory tests and clinical observations for assessing the reliability of innovative dental structures and providing a thorough understanding in the bridge characteristics, e.g. spatial stress distributions, failure modes and failure locations.

### Acknowledgements

This study has been partially supported by Nulite System International Pty. Ltd. Special thanks are due to Dr. Graham Culy from the University of Melbourne for providing the original dental bridge models. Also, the authors are grateful to the anonymous referees and the editor-in-chief for their constructive comments on an early version of the paper.

### References

- [1] Knight GM. The immediate cantilever resin bridge. *Aust Dent Assoc News Bull* 1993;206:26–9.

- [2] Culy G, Tyas MJ. Direct resin-bonded, fibre-reinforced anterior bridges: a clinical report. *Aust Dent J* 1998;43:1–4.
- [3] Li W, Swain MV, Li Q, Ironside J, Steven GP. Fibre reinforced composite dental bridge. Part I: experimental investigation. *Biomaterials*, this issue.
- [4] Grajower R, Stern N, Zamir ST, Kohavi D. Temporary space maintainers retained with composite resin. Part II: fracture load in vitro. *J Prosthet Dent* 1981;45:49–51.
- [5] Altieri JV, Burstone CJ, Jon Goldberg A, Patel AP. Longitudinal clinical of fibre-reinforced composite fixed partial dentures: a pilot study. *J Prosthet Dent* 1994;71:16–22.
- [6] Farah JW, Craig RG, Meroueh KA. Finite element analysis of three- and four-unit bridges. *J Oral Rehab* 1989;16:603–11.
- [7] Yang HS, Thompson VP. A two-dimensional stress analysis comparing fixed prosthodontic approaches to the titled molar abutment. *Int J Prosthodontics* 1991;4:416–24.
- [8] Awadalla HA, Azarbal M, Ismail YH, El-Ibiari W. Three-dimensional finite element stress analysis of a cantilever fixed partial denture. *J Prosthet Dent* 1992;68:243–8.
- [9] Yang HS, Chung HJ, Park YJ. Stress analysis of a cantilevered fixed partial denture with normal and reduced bone support. *J Prosthet Dent* 1996;76:424–30.
- [10] Ash MM, editor. *Wheeler's atlas of tooth form*, 5th ed. Philadelphia: WB Saunders Co.; 1984.
- [11] Choi BK. *Surface modelling for CAD/CAM*. New York: Elsevier Science Publisher; 1991.
- [12] American Dental Association. *Guide to dental materials and devices*, 6th ed. Chicago: American Dental Association; 1972. p. 53.
- [13] Li W. *Finite element analysis for dental bridge and elastic contact design*. PhD thesis. Sydney: The University of Sydney; 2001.
- [14] G+D Computing. *Using Strand7*. Sydney: G+D Computing Pty. Ltd.; 2002.
- [15] Tylman SD, Malone WPF. *Tylman's theory and practice of fixed prosthodontics*, 7th ed. St. Louis: CV Mosby Co.; 1978.
- [16] Darendeliler S, Darendeliler H, Kinoglu T. Analysis of a central maxillary incisor by using a three-dimensional finite element method. *J Oral Rehab* 1992;19:371–83.
- [17] Daniel IM, Ishai O. *Engineering mechanics of composite materials*. New York: Oxford University Press; 1994.
- [18] Anusavice KJ, Hojjatie B. Influence of incisal length of ceramic and loading orientation on stress distribution in ceramic crowns. *J Dent Res* 1988;67:1371–5.
- [19] Beer FP, Johnston Jr ER. *Mechanics of materials*, Si Metric ed. Sydney: McGraw-Hill Pyerson Ltd.; 1987.
- [20] Nulite, Information provided by manufacturer Nulite System International Pty. Ltd. from independent testing, 1995.
- [21] Craig RG. *Restorative dental materials*, 9th ed. St. Louis: CV Mosby Co.; 1993.
- [22] Bayne SC, Taylor DF. *Dental materials*. In: Sturdevant CM, Roberson TM, Heyman HO, Sturdevant JR, editors. *The art and science of operative dentistry*. St. Louis: CV Mosby Co.; 1995. p. 206–87.
- [23] McCormack BAO, Prendergast PJ. Interface failure in implants cemented with different bone-cements—a fracture mechanics analysis. In: Middleton JJML, Pande GN, editors. *Computer methods in biomechanics & biomedical engineering*. London: Gordon and Breach Publishers; 1996. p. 35–45.